Solubility, Activity Coefficients, and Protonation Sequence of Risedronic Acid

ARTICLE *in* JOURNAL OF CHEMICAL & ENGINEERING DATA · NOVEMBER 2014

Impact Factor: 2.04 · DOI: 10.1021/je500621v

4 AUTHORS:

Clemente Bretti
Università degli Studi di Messina
38 PUBLICATIONS **426** CITATIONS
SEE PROFILE

Ignacy Cukrowski
University of Pretoria
102 PUBLICATIONS **986** CITATIONS
SEE PROFILE

Concetta De Stefano
Università degli Studi di Messina
227 PUBLICATIONS **3,067** CITATIONS
SEE PROFILE

Gabriele Lando
Università degli Studi di Messina
37 PUBLICATIONS **232** CITATIONS
SEE PROFILE

Journal of chemical & engineering data

Article

pubs.acs.org/jced

Solubility, Activity Coefficients, and Protonation Sequence of Risedronic Acid

Clemente Bretti,[†] Ignacy Cukrowski,*[,‡] Concetta De Stefano,*[,†] and Gabriele Lando[†]

[†]Dipartimento di Scienze Chimiche, Università degli Studi di Messina, Viale Ferdinando Stagno d'Alcontres, 31, I-98166 Messina, Vill. S. Agata, Italy

[‡]Department of Chemistry, Faculty of Natural and Agricultural Sciences, University of Pretoria, Private Bag X20, Hatfield, 0028, South Africa

ABSTRACT: The solubility and the acid base properties of risedronic acid (RA) were studied in NaCl and $(C_2H_5)_4NI$ aqueous solutions at different ionic strengths and at $T = 298.15 \pm 0.1$ K. The solubility of RA in the two salts is very different; in fact in $NaCl_{(aq)}$ the total solubility increases with increasing salt concentration up to $m_{NaCl} \approx 2$ mol·kg^{-1}. For $m_{NaCl} > 2$ mol·kg^{-1} the solubility slightly decreases, whereas an opposite trend is observed in $(C_2H_5)_4NI_{(aq)}$. The solubility in water is 0.00274 mol·dm^{-3}. From the analysis of the solubility measurements it was possible to determine the Setschenow and the activity coefficients of the neutral species. The four protonation constants of RA were then determined in similar experimental conditions and were analyzed in two ways, considering (i) the variation of the activity coefficients with ionic strength and (ii) the formation of weak complexes between the ions of the supporting electrolytes with the ligand species (a weak complexes model). In the first case, the Debye−Hückel and the specific ion interaction theory were used. The specific interaction and the activity coefficients of the various protonated species were also computed, for example ε (Na^+,RIS^{4-}) = −0.211 ± 0.008 and ε ($(C_2H_5)_4N^+$,RIS^{4-}) = 2.8 ± 0.1. According to the weak complexes model, six species were determined, namely the NaRIS, NaHRIS, NaH_2RIS, NaH_3RIS, Na_2RIS, and Na_2HRIS (RIS = risedronate anion). The protonation sequence of RIS was studied computationally in aqueous environment with explicit water molecules. It was possible to evidence that two tautomers of H_2RIS are formed at approximately 50:50 concentration ratio, and two protons are either placed on two phosphonate groups or distributed between a phosphonate group and a pyridine ring. This finding is important as the HRIS and H_2RIS species are mainly present at the blood plasma pH of 7.4.

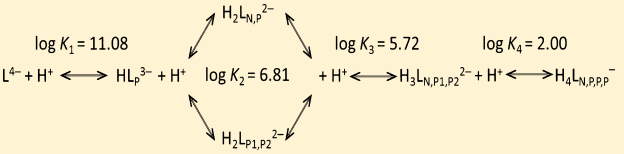

INTRODUCTION

It is generally accepted now that physicochemical effects together with cellular actions must be involved to explain the biological effects of bisphosphonates (BPs) (for excellent reviews on 40 years of studying and medicinal use of BPs, the interested reader is referred to the special issue of *Bone*[10] entitled Bisphosphonates and published in 2011). The duel function of the BPs (see Figure 1) in inhibiting bone resorption, by being selectively taken up and adsorbed to mineral surfaces in bone as well as in interfering with specific biochemical processes, must be accounted for to elucidate and understand their activity and mode of action.

To this effect, the uncertainty related to the degree of protonation of BPs and the placement of protons within a molecule is a serious problem because there is ample evidence in the literature that the charge and proton distributions are linked with the BPs activity, mode of action, etc. For instance, from studies of binding affinities of clinically used BPs to hydroxyapatite it has been concluded that the variation in zeta potential and interfacial tension can be best explained by "*molecular charges related to the protonation of their side-chain moieties, with risedronate showing substantial differences from alendronate, ibandronate, and zoledronate*"[1] and it was suggested that "*differences in kinetic binding affinities, HAP zeta potentials, and interfacial tension are likely to contribute to the biological properties of the various bisphosphonates*".[1] Ironside et al.[2] have used solid-state NMR to study alendronate, pamidronate, neridronate, zoledronate, and tiludronate in their crystalline forms as well as bound to the surface of pure bone mineral stripped of its organic matrix. They found that both the chemical shift anisotropy and asymmetry (obtained for all the studied mineral-bound BPs) cluster in the same anisotropy−asymmetry space as expected for the fully deprotonated state even though solutions adjusted to pH ∼ 7 were allowed to

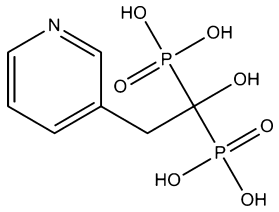

Figure 1. Structure of risedronic acid (RA).

Received: July 3, 2014
Accepted: September 9, 2014
Published: September 22, 2014

interact with the solid bone mineral. A very different model was proposed from the study of interactions of BPs with bone by isothermal titration calorimetry.[3] It has been assumed that the diprotic form of BPs present in a solution (involving one $-PO_3H^-$ group and a protonated amino group of, for example, the aliphatic side chain in the case of alendronate and pamidronate) is preserved after binding to bone. This assumption was used to rationalize the calculated differences in the ΔG, ΔH, and ΔS values obtained for different BPs in terms of pK_a values. The larger ΔG value of the binding of alendronate and pamidronate to bone was attributed to electrostatic interactions between the positively charged protonated side chain of these two BPs and bone. The smallest ΔG value obtained for risedronate was attributed to the pK_a value of pyridine (~5.5) from which they concluded that the side chain in risedronate is only weakly protonated. Interestingly, the pK_a values of imidazol and pyridine were used for zoledronic and risedronic acids, respectively, instead of the experimentally determined protonation constants.

It was suggested[4,5] that the N atom containing bisphosphonates (N-BPs) might be acting as analogues of the carbocation transition state of the enzyme-catalyzed reaction.[6] The carbocation transition state of N-BPs implies that the N atom of the side chain is protonated (hence positively charged) at physiological pH. Since the diprotic form of BPs is the predominant form at blood plasma pH the carbocation analogue must possess two phosphonate groups carrying three negative charges and this was found to be essential for strong binding to FDP synthase.[7,8] On the basis of these findings and to gain further insight into the mechanism of action of the N-BP drugs, Hounslow et al.[9] have investigated the protonation of risedronate and its analogues using NMR-pH titrations. From the determined microprotonation constants, they have concluded that there are two diprotic forms of risedronic acid (RA) at physiological pH in about a 50:50 molar ratio and they involve either a pyridine ring and one phosphonate group or two phosphonate groups.

It is also known that during the process of bone resorption, the subcellular space beneath the osteoclast is significantly acidified.[10] Hence this must have significant influence on the degree of protonation of BPs which are selectively adsorbed to bone mineral at the sites of bone resorption where the mineral is most exposed.[11]

The above clearly demonstrates (i) the importance of knowing which protonated form of a BP is formed (reliable protonation/dissociation constants are required) and protonation sequence (structural placement of protons must be known because this will influence the intramolecular charge distribution and hence the activity of BPs and their mode of action with the immediate chemical and biochemical environment) and (ii) that there is no certainty at all as to the protonation sequence of BPs. Surprisingly, there are relatively few reports on protonation/dissociation constants of BPs[1,9,12−21] and unfortunately, the reported data are highly inconsistent. Not only do the reported values of protonation or dissociation constants vary significantly (sometimes by 2 log units which results in very different pH-distribution of the BPs protonated forms) but also the number of reported constants for the same BP differs. For instance, only three dissociation constants were reported for zoledronate, risedronate, and alendronate.[1] However, four constants were reported for pamidronate[16−19] and risedronate[9] and five constants were reported for pamidronate[15] and alendronate.[14,15]

There are two major aims of this work, namely (i) to establish solubility data and protonation/dissociation constants of risedronic acid RA (Figure 1) of high precision and accuracy and (ii) to propose the most likely protonation sequence of RA from computational modeling.

EXPERIMENTAL SECTION

Chemicals. Risedronic acid solutions were prepared by weighing risedronic acid monohydrate, 99 %, supplied by Hehui Chemical Co., Limited, P.R. China. The resultant concentrations were checked potentiometrically by alkalimetric titrations. Hydrochloric acid (HCl), tetraethylammonium hydroxide $(C_2H_5)_4NOH$ and sodium hydroxide (NaOH) solutions were prepared by diluting concentrated stock solutions (ampules from Sigma-Aldrich). The HCl, $(C_2H_5)_4NOH$ and NaOH solutions were standardized against sodium carbonate and potassium hydrogen phthalate, respectively, previously dried in an oven at T = 383.15 ± 0.1 K for 2 h. Sodium chloride (NaCl) aqueous solutions were prepared by weighing the pure salt dried in an oven at T = 383.15 ± 0.1 K for 2 h. A $(C_2H_5)_4NI$ aqueous solution was prepared by weighing out the salt which was purified as reported by Perrin et al.[22] All solutions were prepared with analytical grade water (R = 18 MΩ·cm^{-1}) using grade A glassware.

Apparatus and Procedure for Potentiometric Measurements. All potentiometric titrations, at ionic strengths 0.110 mol·dm^{-3} ≤ c_{NaCl} ≤ 4.844 mol·dm^{-3} and 0.116 mol·dm^{-3} ≤ $c_{(C_2H_5)_4NI}$ ≤ 0.801 mol·dm^{-3}, were performed at T = 298.15 ± 0.1 K in thermostated cells and at p = 0.1 MPa. To avoid systematic errors and to check the repeatability of data collected, the titrations were performed by two operators on two different experimental setups; the apparatus used has been described in detail elsewhere.[23,24] In each experiment, 25 cm^3 of the titrand solution was titrated with a NaOH or $(C_2H_5)_4NOH$ standardized solution. The titrand solutions contained the ligand (0.003 ≤ c_{RA}/mol·dm^{-3} ≤ 0.020) in the required ionic medium. For each experiment, independent potentiometric titrations of a standardized strong acid−strong base solution were performed at the same conditions as used for the systems under investigation, to determine the standard electrode potential (E^0) and the acidic junction potential ($E_j = j_a \cdot [H^+]$). In this way, the pH scale used was the free scale, pH ≡ $-\log_{10}[H^+]$, where $[H^+]$ is the free proton concentration. For each titration, 80 to 100 data points were collected and the equilibrium state throughout titrations was checked by adopting usual precautions (e.g., by checking the time required to reach an equilibrium and performing back-titrations). For measurements performed at low ionic strengths, the contribution of the ligand to the total ionic strength was considered.

Apparatus and procedure for solubility measurements. The procedure and the theoretical basis of the solubility measurements were described in detail previously.[25,26] Briefly, saturated solutions of RA were prepared by adding an excess of a solid risedronic acid to either NaCl or $(C_2H_5)_4NI$ aqueous solutions with the predetermined ionic strength values (0 < c_{NaCl}/mol·dm^{-3} ≤ 5.0 and 0 < $c_{(C2H5)4NI}$/mol·dm^{-3} ≤ 1.0). The solutions were stirred at T = 298.15 ± 0.1 K for at least 24 h. Preliminary tests confirmed that longer equilibration time was unnecessary. A 25 cm^3 aliquot of the filtered solution (0.45 μm Albet cellulose acetate filters were used) was titrated with the standardized NaOH or $(C_2H_5)_4NOH$ titrant solutions; the same procedure as reported

dx.doi.org/10.1021/je500621v | J. Chem. Eng. Data 2014, 59, 3728−3740

Table 1. Experimental Total Solubility of RA and Solubility of the Neutral Species H_4L^0, both in the Molar and Molal Concentration Scales in the Aqueous NaCl Medium at T = 298.15 ± 0.1 K and p = 0.1 MPa

I/mol·dm^{-3}	log S_c^T	log S_c^0	I/mol·kg^{-1}	log S_m^T	log S_m^0
0.006	−2.565 ± 0.003[a]	−3.369 ± 0.007[a]	0.006	−2.564	−3.368
0.006	−2.565 ± 0.003	−3.350 ± 0.007	0.006	−2.564	−3.349
0.006	−2.568 ± 0.003	−3.341 ± 0.007	0.006	−2.567	−3.340
0.110	−2.481 ± 0.002	−3.181 ± 0.007	0.111	−2.480	−3.179
0.110	−2.499 ± 0.002	−3.228 ± 0.007	0.111	−2.498	−3.227
0.110	−2.501 ± 0.002	−3.234 ± 0.007	0.111	−2.500	−3.232
0.499	−2.378 ± 0.003	−2.858 ± 0.014	0.505	−2.373	−2.853
0.499	−2.375 ± 0.003	−2.853 ± 0.014	0.505	−2.371	−2.849
0.951	−2.332 ± 0.003	−2.811 ± 0.018	0.971	−2.324	−2.803
0.951	−2.327 ± 0.003	−2.801 ± 0.018	0.971	−2.319	−2.792
2.818	−2.346 ± 0.003	−2.709 ± 0.013	2.992	−2.320	−2.683
2.818	−2.344 ± 0.003	−2.709 ± 0.013	2.992	−2.318	−2.683
2.841	−2.336 ± 0.003	−2.710 ± 0.013	3.018	−2.310	−2.685
2.841	−2.329 ± 0.003	−2.710 ± 0.013	3.018	−2.303	−2.685
3.800	−2.378 ± 0.003	−2.849 ± 0.015	4.130	−2.342	−2.814
3.800	−2.376 ± 0.003	−2.849 ± 0.015	4.130	−2.340	−2.814
4.793	−2.444 ± 0.005	−3.013 ± 0.025	5.344	−2.397	−2.966
4.844	−2.473 ± 0.005	−3.177 ± 0.025	5.408	−2.426	−3.129
4.844	−2.473 ± 0.005	−3.177 ± 0.024	5.408	−2.426	−3.129

[a]Value is ± 95 % Confidence Interval (C.I.).

Table 2. Experimental Total Solubility of RA and Solubility of the Neutral Species H_4L^0, both in the Molar and Molal Concentration Scales in the Aqueous $(C_2H_5)_4NI$ Medium at T = 298.15 ± 0.1 K and p = 0.1 MPa

I/mol·dm^{-3}	log S_c^T	log S_c^0	I/mol·kg^{-1}	log S_m^T	log S_m^0
0.116	−2.577 ± 0.003[a]	−3.296 ± 0.010[a]	0.119	−2.567 ± 0.003[a]	−3.286 ± 0.010[a]
0.116	−2.580 ± 0.003	−3.281 ± 0.010	0.119	−2.569 ± 0.003	−3.270 ± 0.010
0.197	−2.565 ± 0.003	−3.269 ± 0.013	0.205	−2.548 ± 0.003	−3.252 ± 0.013
0.197	−2.563 ± 0.003	−3.267 ± 0.013	0.205	−2.546 ± 0.003	−3.250 ± 0.013
0.474	−2.587 ± 0.003	−3.341 ± 0.014	0.521	−2.546 ± 0.003	−3.301 ± 0.014
0.474	−2.587 ± 0.003	−3.344 ± 0.014	0.521	−2.547 ± 0.003	−3.304 ± 0.014
0.562	−2.622 ± 0.005	−3.352 ± 0.012	0.629	−2.574 ± 0.005	−3.304 ± 0.012
0.801	−2.674 ± 0.003	−3.366 ± 0.013	0.942	−2.604 ± 0.003	−3.296 ± 0.013
0.801	−2.674 ± 0.005	−3.371 ± 0.013	0.942	−2.604 ± 0.005	−3.301 ± 0.013
0.801	−2.676 ± 0.005	−3.377 ± 0.013	0.942	−2.607 ± 0.005	−3.307 ± 0.013

[a]Value is ± 95 % C.I.

for the potentiometric measurements was followed. To avoid systematic errors, independent experiments were performed at least three times.

Computational Details. Molecular modeling was performed with the aid of the Gaussian 09, revision B.01, software package.[27] GaussView 5.09[28] was utilized for molecular visualization and construction purposes. Molecules were optimized at the RB3LYP/6-311++G(d,p) level of theory.[29−31]

Optimization of RA was performed with a single spin multiplicity. The structural and electronic properties of each protonated conformer of RA were investigated in water as a solvent (ε = 78.39) using the polarizable continuum model (PCM) and universal force field (UFF) atomic radii (a default solvation model in Gaussian). Frequency calculations were performed by determining analytically the second derivatives of the RB3LYP potential energy surfaces with respect to the fixed atomic nuclear coordinates to determine whether each of the minimized structures corresponded to an energy minimum or a saddle point. All reported geometries belong to genuine minimum energy conformations (imaginary frequencies are not present). Conformational search was performed using Spartan'10, version 1.1.0.[32]

Calculations. The computer programs utilized in this work were reviewed in refs 33 and 34; the ESAB2M program was used to refine all the parameters of the acid−base potentiometric titrations (E^0, K_w, liquid junction potential coefficient, j_a, and analytical concentration of reagents), whereas the BSTAC and STACO programs were used in the calculation of complex formation constants.

All equilibria described in this paper are expressed with the following equations:

$$H^+ + H_{i-1}L^{(i-5)} = H_iL^{(i-4)}K_i \quad (1)$$

or

$$i\,H^+ + L^{4-} = H_iL^{(i-4)}\beta_i \quad (2)$$

where L stands for risedronate anion (RIS). Throughout the paper, uncertainties are given as standard deviation. The conversion from the molar to the molal concentration scale was performed using the appropriate density values.[35]

dx.doi.org/10.1021/je500621v | J. Chem. Eng. Data 2014, 59, 3728−3740

RESULTS AND DISCUSSION

Solubility of Risedronic Acid in NaCl and $(C_2H_5)_4NI$ Aqueous Ionic Media. In previous papers,[25,26] the theoretical aspects of solubility measurements were already reported. Briefly, because of the proton dissociation or association reaction, eq 1 in which the ligand is involved, the total solubility (S^T) of RA is the result of the summation of the concentrations of all the species formed and can be expressed as

$$S^T = [L^{4-}] + [HL^{3-}] + [H_2L^{2-}] + [H_3L^{-}] + [H_4L^0] \quad (3)$$

If H_4L^0 is denoted as the solubility of the neutral species of RA, S^0, and considering the stepwise protonation constants (K_i^H, see hereafter) calculated under the same experimental conditions as used for the solubility measurements, rearrangement of eq 3 leads to

$$S^T = S^\circ \cdot [\sum_0^{4-1} (\prod_4^i K_i \cdot [H^+]^{4-i+1})^{-1}] \quad (4)$$

which can be conveniently used to calculate the solubility of the neutral species from measurements of the total solubility, the pH, and the stepwise protonation constants of RA.

The results of the solubility measurements in the presence of the NaCl and $(C_2H_5)_4NI$ salts are listed in Tables 1 and 2 in which the total solubility and the solubility of the neutral species are reported in the molar (subscript "c") and in the molal (subscript "m"), concentration scales. It was found that the total solubility decreases with an increase in the $(C_2H_5)_4NI$ concentration, whereas the opposite trend is observed in the NaCl aqueous medium up to $m_{NaCl} \sim 2$ mol·kg^{-1}.

For comparison, the total solubility of RA in the two ionic media is shown in Figure 2.

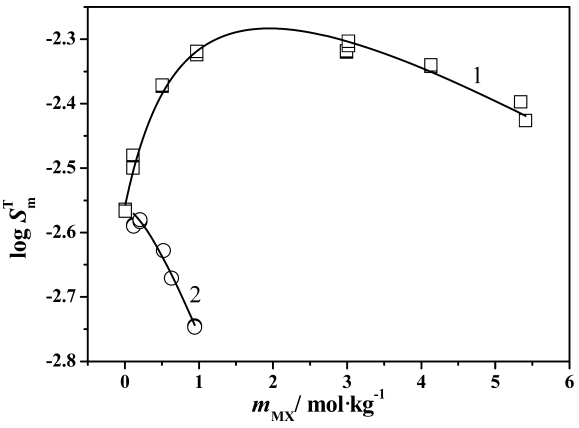

Figure 2. Dependence of the total solubility of risedronic acid on the molal concentration of the background salt at T = 298.15 ± 0.1 K: NaCl (□) and $(C_2H_5)_4NI$ (○).

These data were then analyzed to determine the activity coefficient of the neutral as well as the charged species of RA. The total solubility in the presence of a background salt (log S_m^T) can be expressed as a function of this salt concentration (m_{MX}) according to the following equation

$$\log S_m^T = \log S_{m0}^T + \left(a_\infty + \frac{a_0 - a_\infty}{1 + m_{MX}}\right) m_{MX} \quad (5)$$

where log $S_{m,0}^T$ is the total solubility in pure water and a_0 and a_∞ are empirical parameters. According to Long and McDevit,[36] using the Setschenow constant k_m,[37] variation in the activity coefficient with a background salt concentration is

$$\log \gamma = \log \frac{S_{m0}^0}{S_m^0} = k_m m_{MX} \quad (6)$$

therefore

$$\log S_m^0 = \log S_{m0}^0 - k_m m_{MX} \quad (7)$$

According to the previous report,[38] k_m can be either a true constant or it may vary with ionic strength. In this work, it was found that k_m varies and the following equation was used to describe its dependence on the ionic strength

$$k_m = \left(k_m^\infty + \frac{k_m^0 - k_m^\infty}{m_{MX} + 1}\right) \quad (8)$$

All the parameters of eqs 5,7, and 8, determined here for $NaCl_{(aq)}$ and $(C_2H_5)_4NI_{(aq)}$, are listed in Table 3.

The activity coefficient of the neutral species can be calculated at different salt concentrations by substituting these parameters in eq 6. The variation in the activity coefficient of the H_4L^0 species with the background salt concentration (see Figure 3) also shows an opposite trend for the two salts examined.

Protonation Constants of Risedronic Acid in NaCl and $(C_2H_5)_4NI$ Aqueous Ionic Media. Protonation constants of risedronic acid, determined by potentiometric titrations at different ionic strengths (in the molar and molal concentration scales), are reported in Table 4 (in the NaCl aqueous medium) and Table 5 (in the $(C_2H_5)_4NI$ aqueous medium; all data from the BSTAC computer program).

In Figure 4, the experimental points of two titrations of risedronic acid in $NaCl_{(aq)}$ (□, I = 2.005 mol·dm^{-3}) and $(C_2H_5)_4NI_{(aq)}$ (○, I = 0.801 mol·dm^{-3}) are shown at c_{RA} = 2 mmol dm^{-3} and T = 298.15 ± 0.1 K. To allow the best comparison, the pH values of the solution are reported instead of the emf readings, and the millimoles of added OH^- are reported instead of the amounts of standard base. As it can be observed the pH of the titration in $(C_2H_5)_4NI_{(aq)}$ is always higher than that in $NaCl_{(aq)}$, indicating a stronger association

Table 3. Ionic Strength Dependence Parameters of Total Solubility and Solubility of Neutral Species H_4L^0 in Different Ionic Media in the Molar and in the Molal Concentration Scale at T = 298.15 ± 0.1 K and p = 0.1 MPa

		NaCl		$(C_2H_5)_4NI$	
		p^∞	p^0	p^∞	p^0
log $S_{c0}^{T\,b,c}$	−2.562 ± 0.007[a]	−0.095 ± 0.009[a]	0.581 ± 0.034[a]	−0.392 ± 0.080[a]	0.064 ± 0.036[a]
log $S_{m0}^{T\,b}$	−2.563 ± 0.007	−0.074 ± 0.005[b]	0.569 ± 0.022	−0.233 ± 0.032	0.136 ± 0.034
log $S_{c0}^{0\,c,d}$	−3.352 ± 0.007	0.255 ± 0.023	−1.573 ± 0.040	0.553 ± 0.125	−0.375 ± 0.091
log $S_{m0}^{0\,d}$	−3.353 ± 0.007	0.214 ± 0.020	−1.525 ± 0.038	0.317 ± 0.097	−0.386 ± 0.084

[a]Value is 95 % C.I. [b]Parameter of eq 5. [c]In the molar concentration scale. [d]Parameter of eq 7.

dx.doi.org/10.1021/je500621v | J. Chem. Eng. Data 2014, 59, 3728−3740

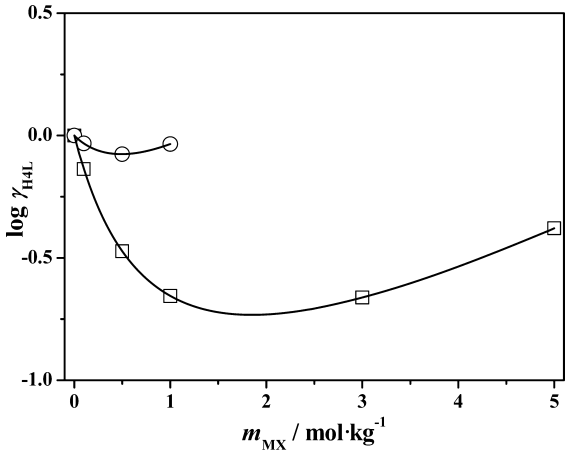

Figure 3. Variation in the activity coefficients of the H_4L^0 species (eq 6) with the concentration of the background salt at T = 298.15 ± 0.1 K: NaCl (□) and $(C_2H_5)_4NI$ (○).

between the proton H^+ and the risedronate, especially at pH > 7.

The dependence of the stability constants on ionic strength of a medium can be obtained from the simple Debye−Hückel (DH)-type equation

$$\log K_i = \log K_i^0 - 0.51 z^* \mathrm{DH} + f(I) \quad (9)$$

$$\mathrm{DH} = \frac{\sqrt{I}}{1 + 1.5\sqrt{I}} \quad (9a)$$

$$z^* = \sum (\text{charge})^2 \text{reactant} - \sum (\text{charge})^2 \text{product} \quad (10)$$

where K_i is a stepwise formation constant and K_i^0 stands for a stepwise formation constant at infinite dilution. Equation 9 is also valid for the overall equilibrium constants, β_i. The $f(I)$ term is a linear function of an ionic strength and it can be formulated in different ways. The simplest expression for this term is $f(I) = C_iI$, where C_i is the only adjustable parameter and the subscript "i" refers to the ith protonation step. However, in some cases the parameter C_i can be dependent on ionic strength according to different equations.[39] To test this, eq 9 was rearranged to the form

$$\log K_i + 0.51 z^* \mathrm{DH} = \log K_i^0 + f(I) \quad (11)$$

and a good linearity was found, which indicates that the function $f(I) = C_iI$ is applicable to all the protonation steps, both in $NaCl_{(aq)}$ and in $(C_2H_5)_4NI_{(aq)}$.

As a general trend, the values of the protonation constants in $(C_2H_5)_4NI_{(aq)}$ were found to be higher than those obtained in the NaCl aqueous ionic medium and this can be attributed to the interactions between the Na^+ cation and the risedronate ligand. As an example, the trends obtained from eq 11 for the second protonation constant in the two salts are shown at T = 298.15 ± 0.1 K in Figure 5.

The experimental data obtained in the $NaCl_{(aq)}$ and in $(C_2H_5)_4NI_{(aq)}$ media were used to compute, from eq 9, the refined values of (i) protonation constants at infinite dilution as well as (ii) ionic strength dependence parameters, and the results obtained are shown in Table 6. The $f(I)$ term, being in this case an empirical parameter in eq 9, can be simply regarded as the smoothing function of log protonation constants. Infinite dilution protonation constants shown in Table 6 were then used in the successive calculations for different models.

The dependence on ionic strength of protonation constants can be also generated from the SIT model[40−43] and Pitzer equations,[44,45] where interaction coefficients have physical meaning. From a general point of view, the protonation constants of RA can be expressed as a function of activity coefficients as follows

$$\log K_i = \log K_i^0 + \log \gamma_{H^+} + \log \gamma_{H_{i-1}L} - \log \gamma_{H_iL} \quad (12)$$

and the equation used in the SIT treatment of protonation constants at different ionic strengths assumes the form of eq 9, in which

$$f(I) = I\Delta\varepsilon_i \quad (13)$$

where i refers to a consecutive protonation step and ε_i stands for a specific interaction coefficient. In the case of the SIT theory, both protonation constants and concentrations must be given in the molal concentration scale. For example, in the case of the four protonation steps of risedronate, in $NaCl_{(aq)}$ we have

$$\Delta\varepsilon_1 = \varepsilon(H^+, Cl^-) + \varepsilon(Na^+, L^{4-}) - \varepsilon(Na^+, HL^{3-}) \quad (14)$$

$$\Delta\varepsilon_2 = \varepsilon(H^+, Cl^-) + \varepsilon(Na^+, HL^{3-}) - \varepsilon(Na^+, H_2L^{2-}) \quad (14a)$$

Table 4. Overall Experimental Protonation Constants of Risedronic Acid in the Molar Concentration Scale in Aqueous NaCl Medium at T = 298.15 ± 0.1 K and p = 0.1 MPa

I/mol·dm^{-3}	log K_1	log β_2	log β_3	log β_4
0.110	10.96 ± 0.02[a]	17.81 ± 0.02[a]	23.54 ± 0.03[a]	25.54 ± 0.03[a]
0.150	11.08 ± 0.02	17.89 ± 0.02	23.61 ± 0.02	25.61 ± 0.03
0.499	10.49 ± 0.01	17.09 ± 0.01	22.74 ± 0.01	24.94 ± 0.02
0.750	10.32 ± 0.01	16.87 ± 0.01	22.52 ± 0.01	24.65 ± 0.02
0.951	10.32 ± 0.02	16.87 ± 0.01	22.49 ± 0.01	24.61 ± 0.02
2.000	9.95 ± 0.02	16.57 ± 0.01	22.28 ± 0.01	2.445 ± 0.02
2.005	10.03 ± 0.02	16.68 ± 0.01	22.41 ± 0.01	24.47 ± 0.02
2.818	9.95 ± 0.01	16.73 ± 0.01	22.49 ± 0.01	24.91 ± 0.02
2.841	10.13 ± 0.01	16.74 ± 0.01	22.53 ± 0.01	24.70 ± 0.03
3.800	9.92 ± 0.01	16.92 ± 0.01	22.82 ± 0.01	24.86 ± 0.02
4.793	9.86 ± 0.01	17.09 ± 0.02	23.00 ± 0.03	25.27 ± 0.03
4.844	9.82 ± 0.01	17.00 ± 0.02	23.13 ± 0.03	24.95 ± 0.03

[a]Value is ± 95 % C.I.

dx.doi.org/10.1021/je500621v | J. Chem. Eng. Data 2014, 59, 3728−3740

Table 5. Overall Protonation Constants of Risedronic Acid in Aqueous $(C_2H_5)_4NI$ Medium Calculated at the Experimental Molar Concentration Ionic Strength Values with the Variable Ionic Strength File of BSTAC Computer Program at T = 298.15 ± 0.1 K and p = 0.1 MPa

I/mol·dm^{-3}	log K_1	log β_2	log β_3	log β_4
0.116	11.40 ± 0.04[a]	18.34 ± 0.05[a]	24.16 ± 0.05[a]	26.25 ± 0.06[a]
0.197	11.47 ± 0.04	18.38 ± 0.05	24.18 ± 0.05	26.28 ± 0.06
0.480	11.90 ± 0.04	18.85 ± 0.05	24.65 ± 0.05	26.82 ± 0.06
0.481	11.90 ± 0.04	18.85 ± 0.05	24.65 ± 0.05	26.83 ± 0.06
0.562	12.03 ± 0.04	19.00 ± 0.05	24.80 ± 0.05	27.01 ± 0.06
0.801	12.41 ± 0.04	19.42 ± 0.05	25.24 ± 0.05	27.51 ± 0.06

[a]Value is ± 95 % C.I.

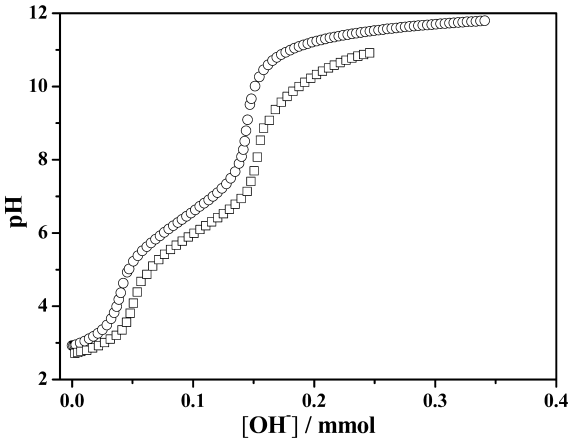

Figure 4. Experimental titrations of risedronic acid in NaCl (□, I = 2.005 mol dm^{-3}) and $(C_2H_5)_4NI$ (○, I = 0.801 mol dm^{-3}) aqueous medium at c_{RA} = 2 mmol dm^{-3} and T = 298.15 ± 0.1 K. The pH of the solution vs equivalents of OH^- added.

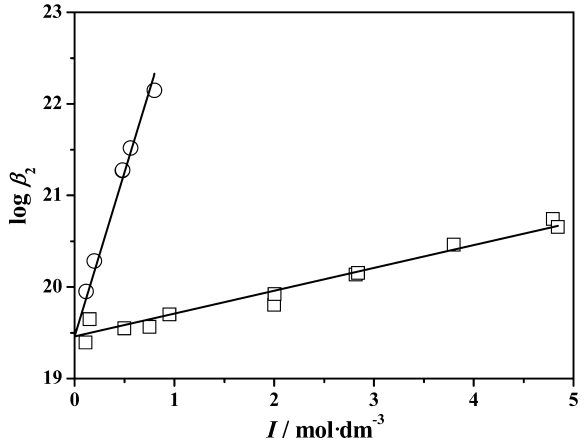

Figure 5. Ionic strength dependence (in the molar concentration scale) of the second protonation constant of risedronic acid in NaCl (□) and in $(C_2H_5)_4NI$ (○) aqueous media at T = 298.15 ± 0.1 K; relationships obtained from eq 11.

$$\Delta\varepsilon_3 = \varepsilon(H^+, Cl^-) + \varepsilon(Na^+, H_2L^{2-}) - \varepsilon(Na^+, H_3L^-) \quad (14b)$$

$$\Delta\varepsilon_4 = \varepsilon(H^+, Cl^-) + \varepsilon(Na^+, H_3L^-) - k_m(H_4L) \quad (14c)$$

The values of the $\Delta\varepsilon_i$ are reported in Table 6. Relevant specific coefficients for the interactions (Na^+,L^{4-}), (Na^+,HL^{3-}), (Na^+,H_2L^{2-}), and (Na^+,H_3L^-) involving different forms of risedronic acid can be obtained by solving the set of eqs 14 to 14c when k_m (Setschenow coefficients reported in Table 5) and $\varepsilon(H^+,Cl^-)$[46] are available. The specific interaction coefficients obtained in this work are presented in Table 7.

As reported in many reviews,[47] many organic ligands form weak complexes with the ions of the supporting electrolytes. In this paper, the interaction of the risedronate ligand with sodium ion was studied in the background of the tetraethylammonium iodide. The theory and the necessary approximation about this consideration are widely reported elsewhere.[48] Briefly, the difference in the ionic strength dependence of the ligand protonation constants in an interacting medium, such as $NaCl_{(aq)}$, and in a neutral (or weakly interacting) ionic medium, such as $(C_2H_5)_4NI_{(aq)}$, can be interpreted in terms of formation of weak complexes between Na^+ and the ligand under study (here RIS). The equation for the dependence of the equilibrium constants on ionic strength is

$$\log K = \log K^0 - z^*\left(\frac{\sqrt{I}}{2 + 3\sqrt{I}}\right) + I(c_1 z^*) \quad (15)$$

where log K^0 and c_1 are the ionic strength dependence parameters and z^* is from eq 10. For the determination of formation constants of weak complexes it is preferred to analyze the data only at I < 1.0 mol·dm^{-3}. This is because the assumption that the activity coefficients of the species are comparable is no longer valid over this limit.

The experimental data obtained in the NaCl and in $(C_2H_5)_4NI$ aqueous media were analyzed with the ES2WC computer program[49] in order to determine (i) the ionic strength dependence parameters, (ii) the protonation constants at infinite dilution, and (iii) the weak complexes formed and their formation constants. Six sodium-containing species with RIS were found, namely NaH_3RIS, NaH_2RIS, NaHRIS, Na_2HRIS, Na_2RIS, and NaRIS. It is widely reported in the literature that the tetraalkylammonium cations can interact with the deprotonated amino group of a molecule; in this case, the aminogroup of the pyridinium residue of the risedronic acid. Hence, the formation of another species, $(C_2H_5)_4NRIS$, was also probed but it was not possible to determine its stability constant. Corrected for the presence of sodium ions (hence accounting for the formation of sodium complexes) the protonation constants for RIS and formation constants for the sodium ion with RIS at infinite dilution and different ionic strengths (obtained for the parameter c_1 = 0.19 ± 0.01) are listed in Table 8.

Data shown in Table 8 indicate that sodium ions have a significant affinity toward RIS which results in the formation of fairly stable complexes which clearly should be accounted for in, for example, blood plasma modeling. One can appreciate the significance of sodium complexes by simply comparing (e.g., at I = 0.5 mol·dm^{-3}) the formation constant of the Na(RIS) (log

dx.doi.org/10.1021/je500621v | J. Chem. Eng. Data 2014, 59, 3728−3740

Table 6. Ionic Strength Dependence Parameters of the Protonation Constants of Risedronate in NaCl and in $(C_2H_5)_4NI$ Aqueous Ionic Media in the Molar and in the Molal Concentration Scale at T = 298.15 ± 0.1 K and p = 0.1 MPa

		NaCl		$(C_2H_5)_4NI$	
i	log $\beta_i^{0a,b}$	C_i^b	$\Delta\varepsilon_i^c$	C_i^b	$\Delta\varepsilon_i^c$
1	11.94 ± 0.06[e]	−0.005 ± 0.009[d]	−0.008 ± 0.005[d]	2.71 ± 0.08[d]	2.39 ± 0.08[d]
2	19.46 ± 0.04	0.247 ± 0.008	0.220 ± 0.004	3.65 ± 0.09	3.19 ± 0.09
3	25.72 ± 0.05	0.420 ± 0.010	0.373 ± 0.005	4.10 ± 0.09	3.55 ± 0.10
4	28.11 ± 0.05	0.484 ± 0.012	0.422 ± 0.003	4.38 ± 0.10	3.72 ± 0.10

[a]In the molal concentration scale this quantity must be corrected log K_c = log K_m − 0.0013p*. [b]Parameter of eq 9. [c]Parameter of eq 13. [d]Value is 95 % C.I.

Table 7. Specific Interaction Coefficients of eqs 14-14c for the H^+/Risedronate System at T = 298.15 ± 0.1 K and p = 0.1 MPa

i	j	$\varepsilon_\infty(i,j)^a$	$\varepsilon_0(i,j)^a$
H^+	Cl^-	0.136[b]	0.0839[b]
H^+	I^-	0.173[b]	0.204[b]
Na^+	L^{4-}	−0.211 ± 0.008[c]	
Na^+	HL^{3-}	−0.078 ± 0.009	
Na^+	H_2L^{2-}	−0.183 ± 0.010	
Na^+	H_3L^{2-}	−0.206 ± 0.009	
H_4L (NaCl)[d]	0.214 ± 0.010[c]	−1.525 ± 0.038[c]	
$(C_2H_5)_4N^+$	L^{4-}	2.849 ± 0.098	
$(C_2H_5)_4N^+$	HL^{3-}	0.648 ± 0.128	
$(C_2H_5)_4N^+$	H_2L^{2-}	0.047 ± 0.141	
$(C_2H_5)_4N^+$	H_3L^{2-}	−0.121 ± 0.146	
H_4L ($(C_2H_5)_4NI$)[d]	0.317 ± 0.097	−0.386 ± 0.084	

[a]Parameter of equation: $\varepsilon = (\varepsilon_\infty + (\varepsilon_0 - \varepsilon_\infty)/(I+1))$. [b]Bretti et al.[46] [c]Value is 95 % C.I. [d]As k_m, eqs 7 to 8.

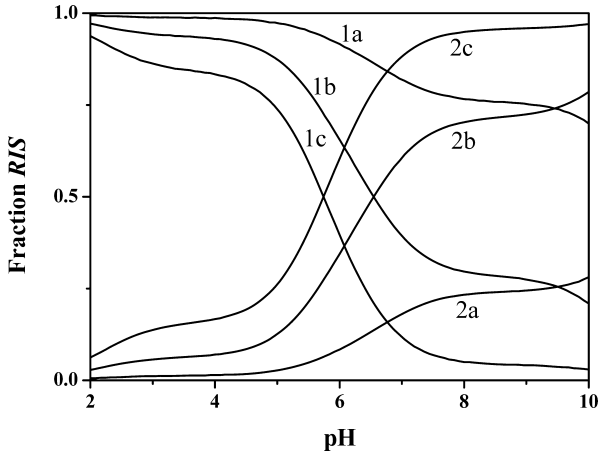

Figure 6. Speciation diagram of the H^+/L^{4-} system in three conditions of NaCl concentrations at T = 298.15 ± 0.1 K: Curve 1, sum of the four protonated species; curve 2, sum of the weak complexes species, "a" refers to I = 0.1 mol·dm^{-3}, "b" is I = 0.5 mol·dm^{-3} and "c" is I = 1.0 mol·dm^{-3}.

K = 1.70 determined here) with that of the Na(EDTA) species (log K = 1.77). Furthermore, in Figure 6 the importance of the sodium complexes is evidenced by the speciation diagrams of the H^+/L^{4-} system for three concentrations of NaCl. Curves marked as 1 and 2 represent the sum of the four protonated ligand species and sodium containing species, respectively. Letters a, b, and c refer to I = 0.1, 0.5, and 1.0 mol·dm^{-3}, respectively. As expected, the amount of relatively weak complexes formed increases with ionic strength and reaches a molar fraction of ∼1 at the I = 1.0 mol·dm^{-3} and pH > 8, indicating that at this ionic strength almost all the risedronate is present in the form of sodium complexes. Also, data shown in Figure 6 predicts that at the blood plasma pH of about 7.4, about 25% of RIS is complexed.

Coming from the above considerations, the description of the H^+/RIS system in $NaCl_{(aq)}$ can be done in two equivalent ways by considering (i) the conditional protonation constants shown in Table 4 and (ii) the protonation constants "purified" of the sodium interactions with RIS by accounting for the formation of six complexes with RIS. From the analysis of the data with the models described above, it was possible to report (Table 9) the suggested values for the risedronate protonation

Table 8. Protonation Constants and Weak Complex Formation Constants between Na^+ and Risedronate at Different Ionic Strengths in the Molar Concentration Scale and at T = 298.15 ± 0.1 K and p = 0.1 MPa

	log β			
equilibrium	I = 0 mol·dm^{-3}	I = 0.1 mol·dm^{-3}	I = 0.5 mol·dm^{-3}	I = 1.0 mol·dm^{-3}
$H^+ + L^{4-} = HL^{3-}$	12.24 ± 0.06[a]	11.54 ± 0.07	11.64 ± 0.08	12.19 ± 0.09
$2\ H^+ + L^{4-} = H_2L^{2-}$	19.67 ± 0.08	18.44 ± 0.09	18.63 ± 0.09	19.59 ± 0.09
$3\ H^+ + L^{4-} = H_3L^-$	25.78 ± 0.09	24.20 ± 0.10	24.44 ± 0.10	25.67 ± 0.10
$4\ H^+ + L^{4-} = H_4L$	28.05 ± 0.10	26.29 ± 0.11	26.56 ± 0.11	27.93 ± 0.12
$Na^+ + L^{4-} = NaL^{3-}$	1.98 ± 0.24	1.28 ± 0.25	1.38 ± 0.26	1.93 ± 0.27
$Na^+ + H^+ + L^{4-} = NaHL^{2-}$	13.25 ± 0.22	12.02 ± 0.23	12.21 ± 0.24	13.17 ± 0.25
$Na^+ + 2\ H^+ + L^{4-} = NaH_2L^-$	20.06 ± 0.21	18.48 ± 0.22	18.72 ± 0.23	19.95 ± 0.24
$Na^+ + 3\ H^+ + L^{4-} = NaH_3L$	25.06 ± 0.40	23.30 ± 0.42	23.57 ± 0.43	24.94 ± 0.44
$2\ Na^+ + L^{4-} = Na_2L^{2-}$	3.28 ± 0.17	2.05 ± 0.18	2.24 ± 0.18	3.20 ± 0.19
$2\ Na^+ + H^+ + L^{4-} = Na_2HL^-$	13.43 ± 0.27	11.85 ± 0.28	12.09 ± 0.28	13.32 ± 0.28

[a]Value is 95 % C.I.

dx.doi.org/10.1021/je500621v | J. Chem. Eng. Data 2014, 59, 3728−3740

Table 9. Suggested Risedronate Protonation Constants in Aqueous NaCl and $(C_2H_5)_4NI$ Media at Different Ionic Strengths (In the Molar and in the Molal Concentration Scales) and at T = 298.15 ± 0.1 K and p = 0.1 MPa

species	salt	I = 0.1	I = 0.5	I = 1.0	I = 3.0	I = 5.0
				Molar Concentration Scale		
HL	NaCl	11.06 ± 0.02[a]	10.54 ± 0.02[a]	10.30 ± 0.02[a]	9.96 ± 0.02[a]	9.82 ± 0.04[a]
	$(C_2H_5)_4NI$	11.34 ± 0.01	11.90 ± 0.01	13.02 ± 0.02		
H_2L	NaCl	17.95 ± 0.02	17.13 ± 0.02	16.85 ± 0.02	16.76 ± 0.03	17.03 ± 0.05
	$(C_2H_5)_4NI$	18.29 ± 0.02	18.83 ± 0.01	20.25 ± 0.01		
H_3L	NaCl	23.79 ± 0.01	22.78 ± 0.01	22.47 ± 0.01	22.56 ± 0.03	23.11 ± 0.06
	$(C_2H_5)_4NI$	24.16 ± 0.01	24.62 ± 0.02	26.15 ± 0.04		
H_4L	NaCl	25.97 ± 0.05	24.85 ± 0.05	24.51 ± 0.04	24.65 ± 0.04	25.29 ± 0.07
	$(C_2H_5)_4NI$	26.36 ± 0.04	26.80 ± 0.04	28.41 ± 0.07		
				Molal Concentration Scale		
HL	NaCl	11.06 ± 0.01	10.53 ± 0.02	10.29 ± 0.03	9.95 ± 0.03	9.82 ± 0.03
	$(C_2H_5)_4NI$	11.31 ± 0.01	11.74 ± 0.03	12.70 ± 0.04		
H_2L	NaCl	17.94 ± 0.01	17.10 ± 0.01	16.79 ± 0.02	16.68 ± 0.02	16.93 ± 0.06
	$(C_2H_5)_4NI$	18.25 ± 0.01	18.60 ± 0.02	19.78 ± 0.05		
H_3L	NaCl	23.78 ± 0.01	22.72 ± 0.02	22.37 ± 0.03	22.39 ± 0.03	22.89 ± 0.07
	$(C_2H_5)_4NI$	24.11 ± 0.01	24.34 ± 0.02	25.58 ± 0.01		
H_4L	NaCl	26.07 ± 0.01	25.18 ± 0.02	24.91 ± 0.03	24.70 ± 0.04	24.74 ± 0.08
	$(C_2H_5)_4NI$	26.32 ± 0.03	26.50 ± 0.05	27.67 ± 0.10		

[a]Value is 95 % C.I.

constants in the NaCl and $(C_2H_5)_4NI$ aqueous media at different ionic strengths and T = 298.15 ± 0.1 K.

Quite surprisingly, the literature findings reporting acid−base properties of RA are only few. In fact, to our knowledge, only Hounslow et al.[9] and Meloun et al.[50] reported protonation constants of this important molecule, and Ebrahimpour et al.[51] reported the solubility data of some biphosphonates (risedronate including). The paper of Hounslow regards the determination of the microscopic equilibrium dissociation constants of risedronate and the role of the nitrogen atom of the 3-picoline residue using NMR and pH titrations. The authors found that the nitrogen atom is partially protonated at the pH of blood plasma and that an H-bond can be formed between the nitrogen of the 3-picoline and the oxygen of the phosphonate group and therefore a proton is shared between the two ionizable groups, populating both the protonic states to have a ∼50:50 distribution between the N- or O-protonated species. This behavior has been proved also in this work by the computational modeling approach, in which 10 explicit water molecules were included in the model. In the paper,[9] the experimental ionic strength at which the dissociation constants were determined is not reported. Considering that the data of Hounslow et al.[9] have been determined at the ionic strength of blood plasma (I = 0.15 mol·dm^{-3}) our results are in a good agreement, in fact log K_2 = 6.81 ± 0.02 and log K_3 = 5.79 ± 0.02 (according to eq 1), compare well with log K_2 = 6.74 and log K_3 = 5.66 reported by Hounslow et al.[9] The paper of Meloun et al.[50] reports a spectrophotometric and potentiometric study of the risedronate protonation equilibria in KCl at different ionic strengths (< 0.2 mol·dm^{-3}) at T = 298.15 ± 0.1 and 310.15 ± 0.1 K. The authors found that at infinite dilution the protonation constants are log K_1 = 12.04 ± 0.05, log K_2 = 7.25 ± 0.02, log K_3 = 6.12 ± 0.02, and log K_4 = 2.48 ± 0.03, and these values slightly decrease with an increase in the temperature. The data reported here, log K_1 = 11.94 ± 0.03, log K_2 = 7.52 ± 0.02, log K_3 = 6.26 ± 0.03, and log K_4 = 2.39 ± 0.03 is in a good agreement with Meloun et al.[50]

Computational Modeling in Simulated Aqueous Environment. There are only two sites where the first proton can be placed, either on the $-PO_3^{2-}$ group (HL_P) or N atom of the pyridine ring (HL_N). All three possible diprotic forms of RA were investigated where the placement of two protons was either on (i) the N atom of the pyridine ring and $-PO_3^{2-}$ group, $H_2L_{N,P}$, (ii) the single $-PO_3^{2-}$ group, $H_2L_{P1,P1}$, or (iii) two $-PO_3^{2-}$ groups, $H_2L_{P1,P2}$. Also, there are three diprotic forms of RA which had to be considered where the placement of two protons was either on (i) the N atom of the pyridine ring and $-PO_3^{2-}$ group, $H_2L_{N,P}$, (ii) the single $-PO_3^{2-}$ group, $H_2L_{P1,P1}$, or (iii) two $-PO_3^{2-}$ groups, $H_2L_{P1,P2}$.

Monoprotic Form of RA. The lowest energy conformer (LEC) of HL_N found after DFT optimization in H_2O as solvent is above 36 kcal·mol^{-1} higher in energy when compared with G(aq) of HL_P Such a large difference in G(aq) clearly indicates, as one would expect, that the only possible in water monoprotic form of RA is HL_P.

Diprotic Form of RA. The differences in G(aq) values were found to be $\Delta G_1(aq) = G_{aq}(H_2L_{N,P}) - G_{aq}(H_2L_{P1,P2}) = \sim 19.2$ kcal·mol^{-1} and $\Delta G_2(aq) = G_{aq}(H_2L_{P1,P1}) - G_{aq}(H_2L_{P1,P2}) = \sim 4.5$ kcal·mol^{-1}; the ΔG(aq) values were calculated using energies of the LECs of each tautomer. Both differences are large and from the Boltzmann distribution in the ΔG(aq) values it follows that only several conformers of the $H_2L_{P1,P2}$ tautomer are predicted to exist in aqueous medium.

Triprotic form of RA. We found that about 50 conformers of the $H_3L_{P1,P1,P2}$ tautomer have lower G(aq) values than the LEC of the $H_3L_{P1,P2,N}$ tautomer. Because of the large population of the $H_3L_{P1,P1,P2}$ conformers, they are predicted to be the only triprotic species of RA even though the energy difference between LECs, $\Delta G(aq) = G_{aq}(H_3L_{N,P1,P2}) - G_{aq}(H_3L_{P1,P1,P2})$, is only 1.97 kcal·mol^{-1}. A much larger difference in G(aq), of about 7 kcal·mol^{-1}, is observed between the LECs of $H_3L_{N,P1,P1}$ and $H_3L_{P1,P1,P2}$ and this strongly indicates that the former is not expected to exist in aqueous medium at all.

From our results it would follow that the protonation sequence in the simulated aqueous environment is HL_P, $H_2L_{P1,P2}$, and $H_3L_{P1,P1,P2}$. The first protonation site could be easily predicted, just from general chemistry knowledge, as involving a $-PO_3^{2-}$ group, and computational data are in full

dx.doi.org/10.1021/je500621v | J. Chem. Eng. Data 2014, 59, 3728−3740

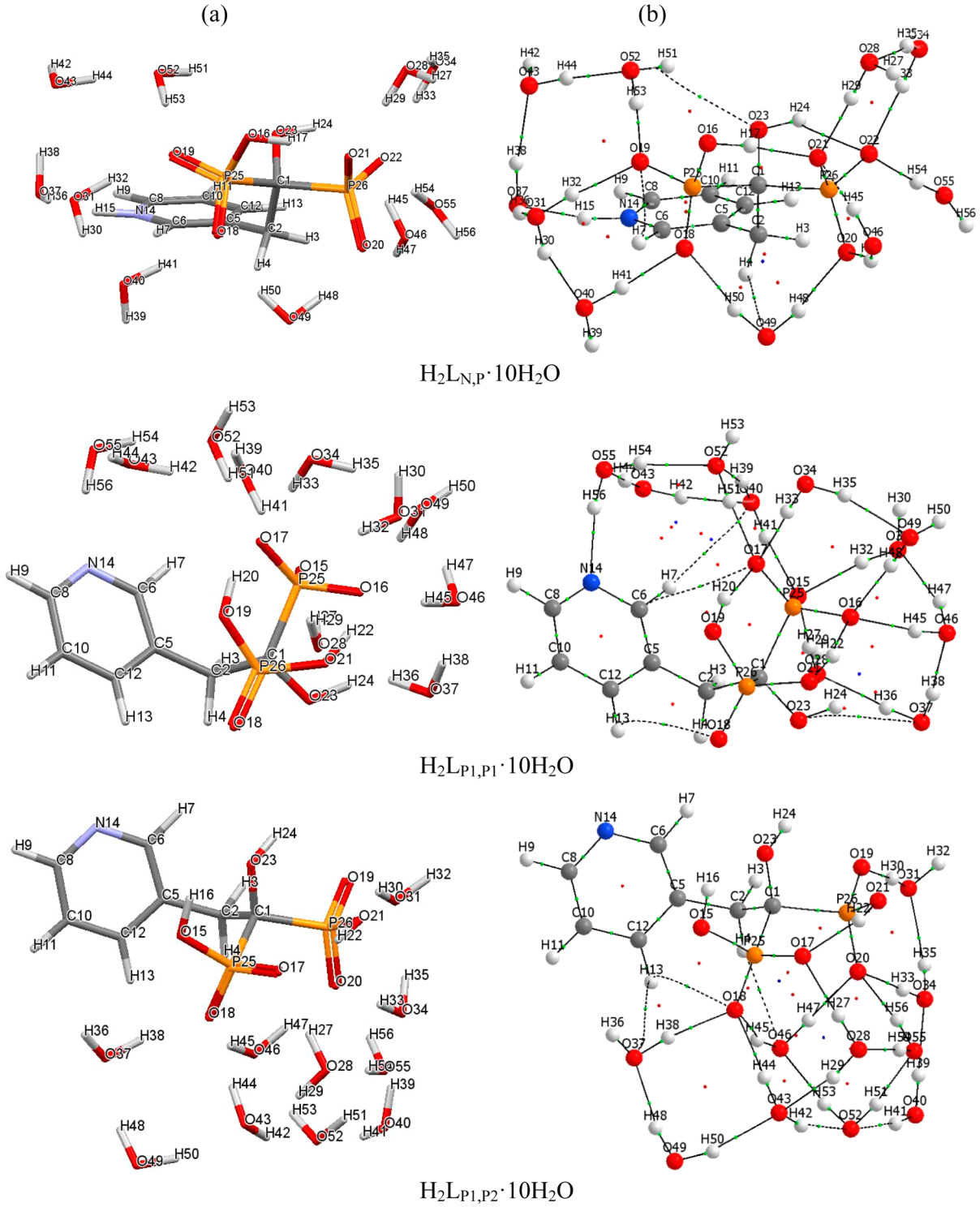

Figure 7. (a) Capped stick representation and (b) molecular graphs of the LECs, G(aq), of the diprotic tautomers of RA·10H_2O.

agreement. However, regarding the diprotic form of RA, our computational modeling predicts that the $H_2L_{N,P}$ tautomer is not formed at all because of its G(aq) value which is larger by about 19 kcal·mol^{-1}. Such a large difference in the free energies between the two tautomers (i) is equivalent to about 14 log units in protonation constants (1.36 kcal·mol^{-1} is equivalent to one protonation constant) and (ii) most likely cannot decrease significantly or change in favor of the $H_2L_{N,P}$ tautomer even when a higher level of theory or another solvation model was used. Unfortunately, this observation contradicts literature reports where the $H_2L_{N,P}$ species was (i) assumed to be present in order to rationalize observed changes in zeta potential of hydroxyapatite (HAP ξ) in the presence of several bisphosphonates at pH $\sim$ 7.4[1] and (ii) proposed to exist in about 50:50 molar ratio with $H_2L_{P1,P2}$ from the analysis of the ^{13}C NMR chemical shifts obtained during NMR−pH titrations on solutions containing RA.[9] Furthermore, even more unexpected is the predicted triprotic tautomer where all three protons are located on the $-PO_3^{2-}$ groups. If one considers, for example, a charge distribution throughout a molecule which

dx.doi.org/10.1021/je500621v | J. Chem. Eng. Data 2014, 59, 3728−3740

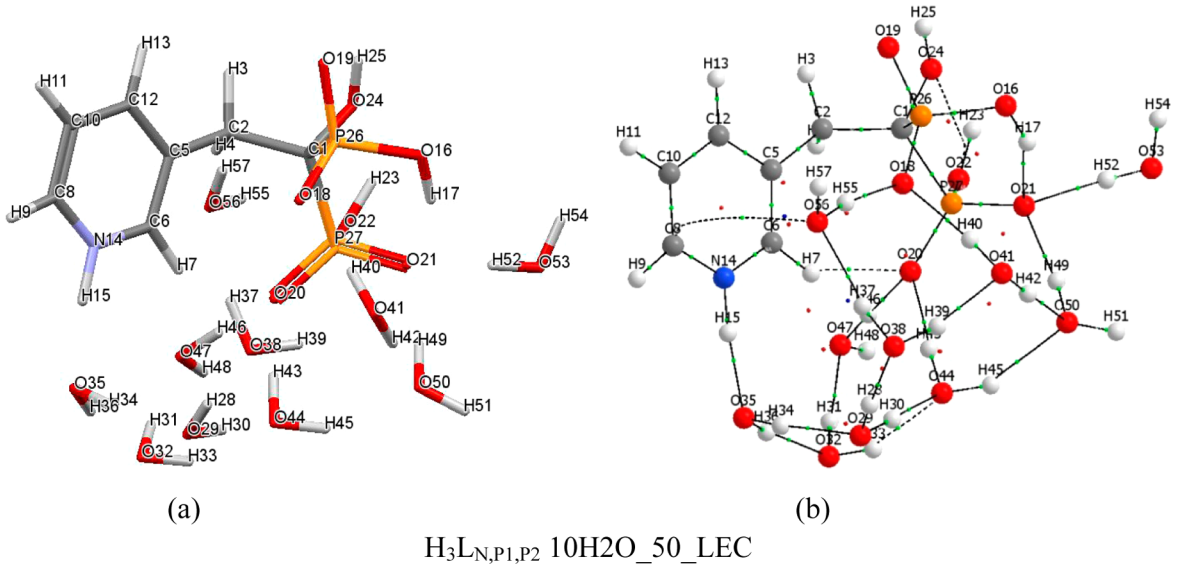

Figure 8. (a) Capped stick representation and (b) molecular graphs of the LEC of $H_3L_{N,P1,P2}$ tautomer of RA optimized with 10 explicit H_2O molecules.

should tend to be as evenly distributed as possible (due to electrostatic forces), then the $H_3L_{N,P1,P2}$ tautomer should be considered as a preferred triprotic form of RA. This reasoning is supported by the fact that the $H_3L_{P1,P1,P2}$ tautomer is not observed in reported crystal structures at all and there exist crystal structures of (1) ammonium risedronate dihydrate,[52] where the $H_3L_{N,P1,P2}$ tautomer is present and (ii) a few metal complexes with RA, where the proton distribution resembles that of the $H_3L_{N,P1,P2}$ tautomer with unprotonated O atoms being involved in the formation of coordination bonds.[13,53]

Clearly, the computational results obtained in the simulated aqueous environment must be of concern, and to address that, we decided to embark on almost an impossible and extremely time-consuming task, namely a DFT-based prediction of the protonation sequence of RA in the presence of explicit water molecules.

Modeling with Explicit Water Molecules. We assumed that to investigate the possibility of N atom being protonated in aqueous solution one must place a sufficient number of water molecules to allow for a necessary intermolecular interaction, >N−H···OH_2. Because RA has two highly negatively charged $-PO_3^{2-}$ moieties, they must be seen as preferential sites for interactions with water molecules. A preliminary, MM-based, conformational search confirmed that fully; when 4 or 6 water molecules were used then they always were placed around the $-PO_3^{2-}$ moieties. Hence, we decided to investigate all possible tautomers of the di- and triprotic forms of RA in the presence of 8 and 10 explicit water molecules. One must realize that the placement of water molecules around the tautomers of RA results in an enormous increase in the degrees of freedom. Furthermore, RA is also a highly flexible molecule which can be present in a number of conformers. Clearly, a large number of possible conformers had to be optimized and it became obvious that a special protocol had to be developed to complete this ambitious project in reasonable time. The scope of this DFT-based modeling is such that it justifies a dedicated communication, and only final outputs obtained in the presence of 10 explicit water molecules will be discussed here.

Diprotic RA·10H_2O. Structures, as capped sticks, and relevant molecular graphs of the LECs of $H_2L_{N,P}\cdot10H_2O$, $H_2L_{P1,P1}\cdot10H_2O$ and $H_2L_{P1,P2}\cdot10H_2O$ are shown in Figure 7. Considering $H_2L_{N,P}\cdot10H_2O$, all deprotonated O atoms of the $-PO_3^{2-}$ groups are involved in two intermolecular H-bonds with surrounding water molecules. Furthermore, the protonated OH groups of the $-PO_3^{2-}$ moieties interact with neighboring deprotonated O atoms rather than with surrounding water molecules. Importantly, the H15-atom of the protonated pyridine ring is involved in the entire intermolecular interaction network.

A preferential formation of intermolecular H-bonds between water molecules and O atoms of $-HPO_3^-$ rather than the unprotonated N atom of the pyridine ring is clearly seen in case of the $H_2L_{P1,P2}\cdot10H_2O$ tautomer. As a matter of fact, only the third conformer of $H_2L_{P1,P2}\cdot10H_2O$ with significantly larger energy (by about 3 kcal·mol^{-1}) shows an interaction involving the N atom. Most likely, in the case of this tautomer, a significantly larger number of water molecules would be required to involve a pyridine ring in intramolecular interaction(s).

Focusing now on the relative energies of the LECs of these tautomers, we obtained $\Delta G_1(aq) = G_{aq}(H_2L_{N,P}\cdot10H_2O) - G_{aq}(H_2L_{P1,P2}\cdot10H_2O) = -0.34$ kcal·mol^{-1} which is a very different result when compared with that obtained without the explicit water molecules. From Boltzmann distribution performed on a number of LECs of all three tautomers it follows that (i) $H_2L_{P1,P1}$ is not formed to any significant extent (%-fraction is much below 1%) and (ii) $H_2L_{N,P}$ and $H_2L_{P1,P2}$ are present in water at almost the same quantity (52.3 and 47.7%, respectively). This is a very gratifying result which not only theoretically confirms the formation of $H_2L_{N,P}$ species at blood plasma pH, as suggested from experimental data,[1,9] but also agrees surprisingly well with a NMR-based quantitative prediction[9] where a marginal dominance of $H_2L_{N,P}$ was obtained from microscopic protonation constants. Furthermore, we can now understand and explain the reported structures of metal complexes, such as $(ZnH_2L_{N,P})_n$ with *R*-factor = 2.58 %[54] or $(CoH_2L_{N,P})_n$ with *R*-factor = 3.46 %.[55] It is obvious that these complexes would not exist in water if the only form of diprotic RA was $H_2L_{P1,P2}$ because, in such a case, it would be impossible to explain the presence of a protonated

dx.doi.org/10.1021/je500621v | J. Chem. Eng. Data 2014, 59, 3728−3740

pyridine ring in these complexes. One can also say that the $H_2L_{N,P}$ species can be seen as a preorganized form of the ligand to form the reported complexes.

Triprotic RA·10H₂O. Considering structural features, they are very much the same as discussed for the diprotic forms of RA, hence we will focus on the relative free energies of the LECs of all three tautomers. $\Delta G_1(aq) = G_{aq}(H_3L_{N,P1,P1}\cdot 10H_2O) - G_{aq}(H_3L_{N,P1,P2}\cdot 10H_2O) = 2.5$ kcal·mol^{-1} and $\Delta G_2(aq) = G_{aq}(H_3L_{P1,P1,P2}\cdot 10H_2O) - G_{aq}(H_3L_{N,P1,P2}\cdot 10H_2O) = 2.9$ kcal·mol^{-1}. From this follows that, opposite to what was predicted from modeling without explicit water molecules, the tautomer with the most even protons distribution, $H_3L_{N,P1,P2}$ (hence also most even charge distribution throughout a molecule) is predicted to be the dominant species in water by far—the LEC of $H_3L_{N,P1,P2}$ is shown in Figure 8. The predicted dominant $H_3L_{N,P1,P2}$ tautomer not only agrees fully with a common chemists' intuition and knowledge but also goes along very well with reported crystal structures of ML_2 complexes, for example, $Ni^{II}(H_3L_{N,P1,P2})_2\cdot 2H_2O$ with *R*-factor = 2.65 %[13] or $Cu^{II}(H_3L_{N,P1,P2})_2\cdot 4H_2O$ with *R*-factor = 3.31 %.[53]

Here again, the dominant $H_3L_{N,P1,P2}$ tautomer can be seen as a preorganized form of the ligand which can instantly coordinate a metal ion without any additional work required to remove a proton.

It is clear that incorporation of explicit water molecules was an absolutely necessary requirement to propose a reliable protonation sequence (it is shown in Figure 9) that fully agrees

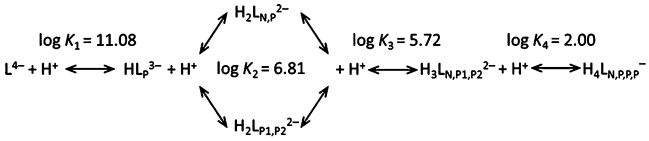

Figure 9. Schematic representation of the protonation sequence of RA at ionic strength of blood plasma (I = 0.15 mol·dm^{-3} and T = 298.15 ± 0.1 K) also showing, as log K values, the stepwise protonation constants.

with all known experimental data. Importantly, from a medicinal point of view (i) at the blood plasma pH of 7.4, the dominant forms of RA are two tautomers, $H_2L_{N,P}$ and $H_2L_{P1,P2}$, with some monoprotic form, HL_P, also present and (ii) in the lower pH range (as expected in the subcellular space beneath the osteoclast, presumably between 3 and 4) the predominant form of RA is $H_3L_{N,P1,P2}$.

CONCLUSIONS

From the analysis of the values of the protonation constants obtained at, for example, I = 0.1 mol·dm^{-3} in $NaCl_{(aq)}$, for (i) risedronate (11.0, 6.8, 5.7, and 2.0 determined in this work), (ii) etidronic acid (10.5, 6.7 and 2.5[56]) and (iii) pyridine is (5.3[57]) it can be presumed that the protonation sequence is P,P,N,P. In this context it is useful to remember that etidronic acid is similar to risedronic acid where the 3-picoline residue is substituted by a methyl.

This work illustrates the usefulness and importance of computational modeling in studying different protonated forms of bisphosphonates in general and RA in particular. It has been demonstrated that in solution, but only when a large number of explicit water molecules was used, there is the possibility of different conformers as well as tautomers RA and this can be attributed to the formation of an extensive network of intra- and intermolecular H-bonds. As an example, it was demonstrated that, in accordance with literature findings,[9] the H_2L^{2-} species is a mixture of the N,P1(52 %) and P1,P2 (48 %) tautomers, which are the predominant species in the blood plasma together with a small amount of HL_P^{3-} species. This is a very important and of general nature issue. For example, in the case of the HL species of a simple amino-acid two protonated species can be formed: the neutral $H_2N-CH-COOH$ and the zwitterionic $H_3N^+-CH-COO^-$; formally the charge is zero for both species, but of course the behavior of the two species is very different.

AUTHOR INFORMATION

Corresponding Authors

*E-mail: ignacy.cukrowski@up.ac.za. Tel: +27 12 420 3988. Fax: +27 12 420 4687.

*E-mail: cdestefano@unime.it. Tel: +39 090 676 5749. Fax: +39 090 392827.

Funding

This work is based on the research supported in part by the National Research Foundation of South Africa (Grant No. 87777) and University of Pretoria. C. Bretti, C. De Stefano and G. Lando thank the University of Messina for partial financial support.

Notes

The authors declare no competing financial interest.

REFERENCES

(1) Nancollas, G. H.; Tang, R.; Phipps, R. J.; Henneman, Z.; Gulde, S.; Wu, W.; Mangood, A.; Russell, R. G. G.; Ebetino, F. H. Novel insights into actions of bisphosphonates on bone: Differences in interactions with hydroxyapatite. *Bone* **2006**, *38*, 617−627.

(2) Ironside, M. S.; Duer, M. J.; S, S. B. Bisphosphonate protonation states, conformations, and dynamics on bone mineral probed by solid-state NMR without isotope enrichment. *Eur. J. Pharm. Biopharm.* **2010**, *76*, 120−126.

(3) Mukherjee, S.; Huang, C.; Guerra, F.; Wang, K.; Oldfield, E. Thermodynamics of bisphosphonates binding to human bone: A two-site model. *J. Am. Chem. Soc.* **2009**, *131*, 8374−8375.

(4) Grove, J. E.; Brown, R. J.; Watts, D. J. The intracellular target for the antiresorptive aminobisphosphonate drugs in Dictyostelium discoideum is the enzyme farnesyl diphosphate synthase. *J. Bone. Miner. Res.* **2000**, *15*, 971−981.

(5) Martin, M. B.; Arnold, W.; Heath, H. T.; Urbina, J. A.; Oldfield, E. Nitrogen-containing bisphosphonates as carbocation transition state analogs for isoprenoid iosynthesis. *Biochem. Biophys. Res. Commun.* **1999**, *263*, 754−758.

(6) Poulter, C. D.; Rilling, H. C. The prenyl transfer reaction. Enzymatic and mechanistic studies of the 1′-4 coupling reaction in the terpene biosynthetic pathway. *Acc. Chem. Res.* **1978**, *11*, 307−313.

(7) Hosfield, D. J.; Zhang, Y.; Dougan, D. R.; Broun, A.; Tari, L. W.; Swanson, R. V. Structural basis for bisphosphonate-mediated inhibition of isoprenoid biosynthesis. *J. Biol. Chem.* **2004**, *278*, 8526−8529.

(8) Tarshis, L. C.; Yan, M.; Poulter, D.; Sacchettini, J. C. Crystal structure of recombinant farnesyl diphosphate synthase at 2.6-Å resolution. *Biochem.* **1994**, *33*, 10871−10877.

(9) Hounslow, A. M.; Carran, J.; Brown, R. J.; Rejman, D.; Blackburn, G. M.; Watts, D. J. Determination of the microscopic equilibrium dissociation constants for risedronate and its analogues reveals two distinct roles for the nitrogen atom in nitrogen-containing bisphosphonate drugs. *J. Med. Chem.* **2008**, *51*, 4170−4178.

(10) Russell, R. G. G. Bisphosphonates: The first 40 years. *Bone* **2011**, *49*, 2−19.

(11) Azuma, Y.; Sato, H.; Oue, Y.; Okabe, K.; Ohta, T.; Tsuchimoto, M.; Kiyoki, M. Alendronate distributed on bone surfaces inhibits

osteoclastic bone resorption in vitro and in experimental hypercalcemia models. *Bone* **1995**, *16*, 235−245.
(12) Boichenko, A. P.; Markov, V. V.; Kong, H. L.; Matveeva, A. G.; Loginova, L. P. Re-evaluated data of dissociation constants of alendronic, pamidronic, and olpadronic acids. *Cent. Eur. J. Chem.* **2009**, *7*, 8−13.
(13) Demoro, B.; Caruso, F.; Rossi, M.; Benitez, D.; Gonzalez, M.; Cerecetto, H.; Parajan-Costa, B.; Castiglioni, J.; Galizzi, M.; Docampo, R.; Otero, L.; Gambino, D. Risedronate metal complexes potentially active against Chagas disease. *J. Inorg. Biochem.* **2010**, *104*, 1252−1258.
(14) Dyba, M.; Jezowska-Bojczuk, M.; Kiss, E.; Kiss, T.; Kozlowski, H.; Leroux, Y.; Manouni, D. E. 1-Hydroxyalkane-1,l-diyldiphosphonates as potent chelating agents for metal ions. Potentiometric and spectroscopic studies of copper(II) coordination. *J. Chem. Soc. Dalton. Trans.* **1996**, 1119−1123.
(15) Hägele, G.; Szakács, Z.; Ollig, J.; Hermens, S.; Pfaff, C. NMR-controlled titrations: Characterizing aminophosphonates and related structures. *Heteroatom. Chem.* **2000**, *11*, 562−582.
(16) Martell, A. E.; Smith, R. M.; Motekaitis, R. J. *NIST Critically selected stability constants of metal complexes database*, 8.0; National Institute of Standard and Technology: Garthersburg, MD, 2004.
(17) May, P. M.; Murray, K. *Joint Expert Speciation System*; Jess Primer: Murdoch, Australia, 2000.
(18) Pettit, D.; Powell, K. K. *Stability Constants Database*; Academic software, IUPAC: Otley, UK, 1997.
(19) Popov, K.; Rönkkömäki, H.; Lajunen, L. H. J. Critical evaluation of stability constants of phosphonic acids. *Pure Appl. Chem.* **2001**, *73*, 1641−1677.
(20) Zeevaart, J. R.; Jarvis, N. V.; Cukrowski, I.; Jackson, G. E. Blood plasma modelling of the in vivo behaviour of bisphosphonate-metal-ion complexes as radiopharmaceuticals. *S. Afr. J. Chem.* **1997**, *50*, 189−194.
(21) Zeevaart, J. R.; Jarvis, N. V.; Louw, W. K. A.; Jackson, G. E.; Cukrowski, I.; Mouton, C. J. Metal-ion speciation in blood plasma incorporating the bisphosphonate, 1-hydroxy-4-amino-propilydenedi-phosphonate (APD), in therapeutic radiopharmaceuticals. *J. Inorg. Biochem.* **1999**, *73*, 265−272.
(22) Perrin, D. D.; Armarego, W. L. F. *Purification of Laboratory Chemicals*, 3rd ed.; Pergamon Press: Oxford (UK), 1988; p 392.
(23) Cigala, R. M.; Crea, F.; De Stefano, C.; Lando, G.; Milea, D.; Sammartano, S. Electrochemical Study on the Stability of Phytate Complexes with Cu^{2+}, Pb^{2+}, Zn^{2+}, and Ni^{2+}: A Comparison of Different Techniques. *J. Chem. Eng. Data* **2010**, *55*, 4757−4767.
(24) Cigala, R. M.; Crea, F.; De Stefano, C.; Lando, G.; Milea, D.; Sammartano, S. Modeling the acid−base properties of glutathione in different ionic media, with particular reference to natural waters and biological fluids. *Amino Acids* **2012**, *43*, 629−648.
(25) Bretti, C.; Crea, F.; De Stefano, C.; Sammartano, S.; Vianelli, G. Some thermodynamic properties of DL-tyrosine and DL-tryptophan. Effect of the ionic medium, ionic strength, and temperature on the solubility and acid−base properties. *Fluid Phase Equilib.* **2012**, *314*, 185−197.
(26) Bretti, C.; De Stefano, C.; Foti, C.; Sammartano, S. Acid-base properties, solubility, activity coefficients, and Na^+ ion pair formation of complexons in $NaCl_{(aq)}$ at different ionic strengths ($0 \le I \le 4.8$ mol L^{-1}). *J. Solution Chem.* **2013**, *42*, 1452−1471.
(27) Frisch, M. J.; Trucks, G. W.; Schlegel, H. B.; Scuseria, G. E.; Robb, M. A.; Cheeseman, J. R.; Scalmani, G.; Barone, V.; Mennucci, B.; Petersson, G. A.; Nakatsuji, H.; Caricato, M.; Li, X.; Hratchian, H. P.; Izmaylov, A. F.; Bloino, J.; Zheng, G.; Sonnenberg, J. L.; Hada, M.; Ehara, M.; Toyota, K.; Fukuda, R.; Hasegawa, J.; Ishida, M.; Nakajima, T.; Honda, Y.; Kitao, O.; Nakai, H.; Vreven, T.; Montgomery, J., J, A.; Peralta, J. E.; Ogliaro, F.; Bearpark, M.; Heyd, J. J.; Brothers, E.; Kudin, K. N.; Staroverov, V. N.; Kobayashi, R.; Normand, J.; Raghavachari, K.; Rendell, A.; Burant, J. C.; Iyengar, S. S.; Tomasi, J.; Cossi, M.; Rega, N.; Millam, N. J.; Klene, M.; Knox, J. E.; Cross, J. B.; Bakken, V.; Adamo, C.; Jaramillo, J.; Gomperts, R.; Stratmann, R. E.; Yazyev, O.; Austin, A. J.; Cammi, R.; Pomelli, C.; Ochterski, J. W.; Martin, R. L.; Morokuma, K.; Zakrzewski, V. G.; Voth, G. A.; Salvador, P.; Dannenberg, J. J.; Dapprich, S.; Daniels, A. D.; Farkas, Ö.; Foresman, J. B.; Ortiz, J. V.; Cioslowski, J.; Fox, D. J. *Gaussian 09*, revision B.01; Gaussian, Inc.: Wallingford, CT, 2010.
(28) Dennington, R.; Keith, T.; Millam, J. *GaussView*, version 5.0.0b; Semichem Inc.: Shawnee Mission, KS, 2009.
(29) Becke, A. D. Density functional thermochemistry. III. The role of exact exchange. *J. Chem. Phys.* **1993**, *98*, 5648−5652.
(30) Lee, C.; Yang, W.; Parr, R. G. Development of the Colle−Salvetti correlation-energy formula into a functional of the electron density. *Phys. Rev. B* **1988**, *37*, 785−789.
(31) Stephens, P. J.; Devlin, F. J.; Chabalowski, C. F.; Frisch, M. J. Ab initio calculation of vibrational absorption and circular dichroism spectra using density functional force fields. *J. Phys. Chem.* **1994**, *98*, 11623−11627.
(32) Wavefunction. *Spartan '10*, 1.1.0; Wavefunction Inc.: Irvine, CA, 2001.
(33) De Stefano, C.; Princi, P.; Rigano, C.; Sammartano, S. Computer analysis of equilibrium data in solution. ESAB2M: An improved version of the ESAB Program. *Ann. Chim. (Rome)* **1987**, *77*, 643−675.
(34) De Stefano, C.; Sammartano, S.; Mineo, P.; Rigano, C., Computer tools for the speciation of natural fluids. In *Marine Chemistry—An Environmental Analytical Chemistry Approach*; Gianguzza, A., Pelizzetti, E., Sammartano, S., Eds.; Kluwer Academic Publishers: Amsterdam, The Netherlands, 1997; pp 71−83.
(35) De Stefano, C.; Foti, C.; Sammartano, S.; Gianguzza, A.; Rigano, C. Equilibrium studies in natural fluids. use of synthetic seawater and other media as background salts. *Ann. Chim. (Rome)* **1994**, *84*, 159−175.
(36) Long, F. A.; McDevit, W. F. Activity coefficients of nonelectrolyte solutes in aqueous salt solutions. *Chem. Rev.* **1952**, *51*, 119−169.
(37) Setschenow, J. Z. Uber die konstitution der salzlosungenauf grund ihres verhaltens zu kohlensaure. *Z. Phys. Chem.* **1889**, *4*, 117−125.
(38) Bretti, C.; Cigala, R. M.; Crea, F.; Foti, C.; Sammartano, S. Solubility and activity coefficients of acidic and basic nonelectrolytes in aqueous salt solutions. 3. Solubility and acitivity coefficients of adipic and pimelic acids in NaCl(aq), $(CH_4)_4NCl$(aq) and $(C_2H_5)_4NI$(aq) at different ionic strengths and at t = 25 °C. *Fluid Phase Equilib.* **2008**, *263*, 43−54.
(39) Bretti, C.; Foti, C.; Sammartano, S. A new approach in the use of SIT in determining the dependence on ionic strength of activity coefficients. Application to some chloride salts of interest in the speciation of natural fluids. *Chem. Spec. Bioavail.* **2004**, *16*, 105−110.
(40) Brönsted, J. N. Studies on solubility IV. Principle of the specific interaction of ions. *J. Am. Chem. Soc.* **1922**, *44*, 887−898.
(41) Grenthe, I.; Puigdomenech, I. *Modelling in Aquatic Chemistry*. OECD-NEA: Paris, France, 1997.
(42) Guggenheim, E. A.; Turgeon, J. C. Specific interaction of ions. *Trans. Faraday Soc.* **1955**, *51*, 747−761.
(43) Scatchard, G. Concentated solutions of strong electrolytes. *Chem. Rev.* **1936**, *19*, 309−327.
(44) Pitzer, K. S. Thermodynamics of electrolytes. I. Theoretical basis and general equations. *J. Phys. Chem.* **1973**, *77*, 268−277.
(45) Pitzer, K. S. *Activity Coefficients in Electrolyte Solutions*. CRC Press: Boca Raton, FL, 1991.
(46) Bretti, C.; Foti, C.; Porcino, N.; Sammartano, S. SIT parameters for 1:1 electrolytes and correlation with Pitzer coefficients. *J. Solution Chem.* **2006**, *35*, 1401−1415.
(47) Daniele, P. G.; Foti, C.; Gianguzza, A.; Prenesti, E.; Sammartano, S. Weak alkali and alkaline earth metal complexes of low molecular weight ligands in aqueous solution. *Coord. Chem. Rev.* **2008**, *252*, 1093−1107.
(48) Bretti, C.; De Stefano, C.; Lando, G.; Sammartano, S. Activity coefficients, acid-base properties, and weak Na^+ ion pair formation of some resorcinol derivatives. *Fluid Phase Equilib.* **2010**, *292*, 71−79.
(49) De Robertis, A.; De Stefano, C.; Sammartano, S.; Rigano, C. The Determination of Formation Constants of Weak Complexes by

Potentiometric Measurements: Experimental Procedures and Calculation Methods. *Talanta* **1987**, *34*, 933−938.
(50) Meloun, M.; Ferenčiková, Z.; Málkova, H.; Pekárek, T. Thermodynamic dissociation constants of risedronate using spectrophotometric and potentiometric pH-titration. *Cent. Eur. J. Chem.* **2012**, *10*, 338−353.
(51) Ebrahimpour, A.; Ebetino, F. H.; Sethuraman, G.; Nancollas, G. H., Determination of solubility and calcium ion stability constants of a phosphonoalkylphosphinate (PAP) and bisphosphonates (BPs) Such as EHDP, risedronate, alendronate, 3-pic AMBP, and 3-pic AMPMP. In *Mineral Scale Formation and Inhibition*; Amjad, Z., Ed.; Springer: New York, 1995; pp 295−305.
(52) Stahl, K.; Oddershede, J.; Preikschat, H.; Fischer, E.; Bennekou, J. S. Ammonium 1-hydroxy-2-(2-pyridinio)ethane-1,1-diyldiphosphonate dihydrate and potassium 1-hydroxy-2-(2-pyridinio)ethane-1,1-diyldiphosphonate dihydrate. *Acta Crystallogr. C* **2006**, *C62*, m112−m115.
(53) Kunnas-Hiltunen, S.; Laurila, E.; Haukka, M.; Vepsalainen, J.; Ahlgren, M. Organic−inorganic hybrid materials: Syntheses, X-ray diffraction study, and characterisations of manganese, cobalt, and copper complexes of modified bis(phosphonates). *Z. Anorg. Allg. Chem.* **2010**, *636*, 710−720.
(54) Huang, X.; Liu, Z.; Huang, C.; Wang, Y. *catena*-Poly[zinc(II)-μ3-{hydrogen [1-hydroxy-2-(3-pyridinio)ethane-1,1-diyl]-diphosphonate}]. *Acta Crystallogr. E* **2010**, *E66*, m59−m60.
(55) Zhang, Z. C.; Gao, S.; Zheng, L. M. Cobalt diphosphonate with a new double chain structure exhibiting field-induced magnetic transition. *Dalton Trans.* **2007**, 4681−4684.
(56) Foti, C.; Giuffrè, O.; Sammartano, S. Thermodynamics of HEDPA protonation in different media and complex formation with Mg^{2+} and Ca^{2+}. *J. Chem. Thermodyn.* **2013**, *66*, 151−160.
(57) Bretti, C.; Cigala, R. M.; De Stefano, C.; Lando, G.; Sammartano, S. Thermodynamics for proton binding of pyridine in different ionic media at different temperatures. *J. Chem. Eng. Data* **2014**, *59*, 143−156.